Numerical investigation of the unsteady flow through a counter-rotating fan

K. Engel M. Faden S. Pokorny
DLR*, Institute for Propulsion Technology
Linder Hoehe
D-5000 Cologne 90, Germany

Abstract

In this paper an interactive flow simulation system for the theoretical investigation of unsteady flow phenomena in turbomachinery components is presented.

The numerical methods employed for the solution of the time dependent Euler equations, the entry and exit boundary formulations and the coupling procedure for relatively moving grids are described.

The application of the system on the simulation of the start-up and acceleration process of two relatively moving cascades is illustrated by figures showing pressure contours at different time levels.

I Introduction

The efforts for increasing the efficiency of civil jet engines leads to a new propulsion concept in the 70's, the so called Propfan. In order to decrease the fan diameter, the fan exit swirl and to maintain the propulsive efficiency on a very high level, Propfan based Ultra-High-Bypass Engines (UHB) are under development. One of these concepts is the counterrotating ducted Propfan engine, i.e. the CRISP concept (Fig. 1).

The institute for propulsion technology of the DLR has been investigating the flow field of an counter-rotating fan theoretical as well as in wind tunnel tests. Contrary to the latter the numerical investigation leads to very 'compact' data. Therefore it is possible to study fundamental physical phenomena.

Following this idea an interactive flow simulation system is under development by the authors to study and analyze the unsteady flow phenomena in turbomachinery. Special emphasis is put on the unsteady effects of the flow through the blades of the counter-rotating ducted fan rotors mentioned above.

The whole system has been setup on a parallel computer which provides the necessary computational power together with the required interactive access.

The system serves as a numerical test facility which allows the user to alter various parameters like rotor-speed

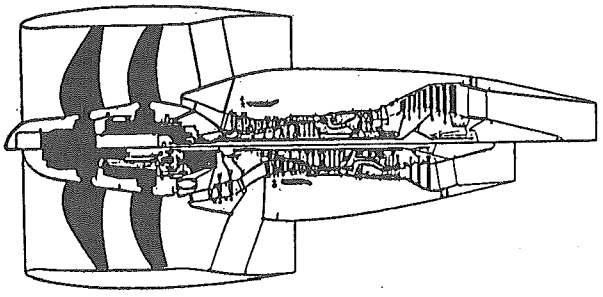

Figure 1: Sectional view of a jet engine with 2 counter-rotating fan-rotors (CRISP-Concept)

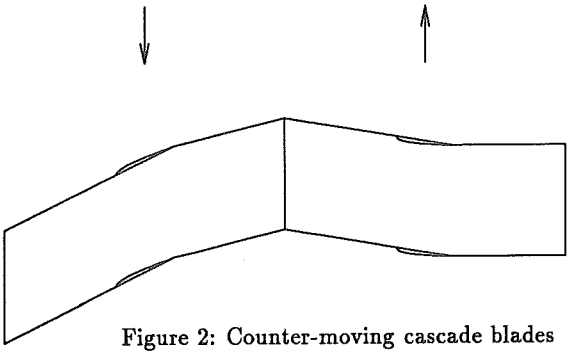

Figure 2: Counter-moving cascade blades

, exit pressure, etc. during runtime of the calculation as well as request information about the current state of the system. Through these features the user has the capability of performing 'numerical experiments' [2].

As a first step towards a 3-D Navier-Stokes code a 2-D Euler code for the calculation of countermoving cascades (Fig. 2) is implemented.

The code is a non-MUSCL explicit TVD scheme based

*German Aerospace Research Establishment

on Roe's approximate Rieman solver [8] and the modified flux approach of Harten [5] and Yee [10].

Since the calculations are carried out on a finite domain, accurate physical and numerical boundary treatments are necessary to avoid non-physical results. Practical formulations which satisfy these requirements are decisive for the simulation system.

The flow mentioned above is characterised by blade interactions which produce periodic unsteady perturbations. These perturbations have to pass the boundaries without any non-physical reflections so that the flow field becomes independent of the boundary location.

In this paper a short survey on the interactive system will be given. Then the used numerical algorithm is described, including the explicit TVD scheme, the fluxlimiter the method of grid coupling and the boundary conditions. In the remaining part the results of the calculation of 2D counter-moving cascades representing a typical transonic near tip section of the blades of the counter-rotating fan will be presented.

II System Description

Today parallel computers use up to hundreds or thousands of nodes (processors) while future systems are expected to increase the number at least one order of magnitude. Thus the key issue in developing code for parallel computers is that it must run on an arbitrary number of processors in order to exploit massive parallel systems effectively. However this does not mean that for a given problem size solely the number of processors must scale keeping the overall performance somewhere acceptable. The use of parallel computers should provide the ability to address problems which probably cannot be solved on existing scalar machines. This implies that a parallel code must run efficiently when the ratio of the number of processors employed over the problem size is kept constant at an as high as possible value.

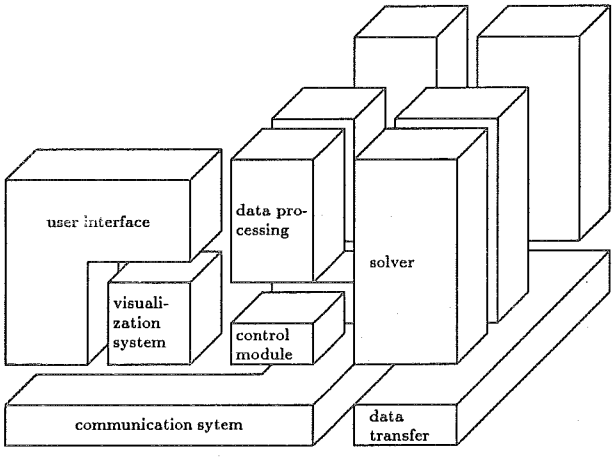

Figure 3: The software layout of the flow simulation system

The single node of a parallel computer is slower than the processor of a supercomputer. Thus not only the processor itself but also its own local memory is cheaper. This in turn means that parallel computers posess not only a higher computational performance but also a larger memory. On the other side the bandwidth to the user interface, usually a graphic workstation, remains constant leading to a possible bottleneck when tackling large problems. Recognizing these points a system consisting of a flow solver plus a visualization system running on a parallel machine has been designed. The overall layout is shown in figure 3. The major components are

Flow Solver An explicit non-MUSCL upwind TVD scheme formulated on general coordinates,

Data Processing A system which allows single modules to be arranged interactively to analyze all desired properties. The system was designed following an initial idea of AVS [12],

Control Module It controls the execution of the flow solver and of the visualisation system. It processes the user commands during run time,

Communication System It distributes the commands and synchronizes all necessary information within the processor network,

Visualization System A module to visualize directly the incoming data from the parallel system. It runs on a graphic workstation,

User Interface A parser that allows commands to be sent interactively to the processor network while the flow solver is running. This parser enables basic syntax checking of commands so that user faults do not corrupt system execution.

The parallel computer and the workstation used for visualization are coupled directly via special hardware to allow fast data transfer.

III The Numerical Algorithm

Currently the upwind TVD scheme for the Euler equations devolped by Harten and Yee[10] using Roe's approximate Riemann solver is implemented. The solver is parallelized using a domain decomposition method [3].

In the following subsections the TVD scheme followed by the currently implemented flux limiter and the grid coupling method used are described. The latter is of special interest since each cascade is calculated using a grid fixed to the local blades. Thus these two relatively moving grids have to be coupled in such a way that there is no additional error introduced into the scheme. Also a short describtion of the used boundary conditions is given.

TVD Scheme The two dimensional Euler equations in general moving coordinates $\xi = \xi(x,y,t), \eta = \eta(x,y,t)$ may be written as

$$\frac{\partial \hat{U}}{\partial t} + \frac{\partial \hat{F}}{\partial \xi} + \frac{\partial \hat{G}}{\partial \eta} = 0 \tag{1}$$

where $\hat{U} = \{\rho, \rho u, \rho v, e\}$ is the conservative variable vector, $\hat{F} = (\xi_x F + \xi_y G + \xi_t U)/J$ and $\hat{G} = (\eta_x F + \eta_y G + \eta_t U)/J$ are the fluxes in ξ and η, respectively. The cartesian fluxes are $F = \{\rho u, \rho u^2 + p, \rho uv, u(e+p)\}$ and $G = \{\rho v, \rho vu, \rho v^2 + p, v(e+p)\}$. The time integration method is a four step Runge-Kutta method which may be written as

$$\begin{aligned} U^0 &= U^n \\ U^1 &= U^0 - \alpha_1 R(U^0) \qquad U^2 = U^0 - \alpha_2 R(U^1) \\ U^3 &= U^0 - \alpha_3 R(U^2) \qquad U^{n+1} = U^0 - \alpha_4 R(U^3) \end{aligned} \tag{2}$$

where $\alpha_1 = 0.091$, $\alpha_2 = 0.24$, $\alpha_3 = 0.42$, and $\alpha_4 = 1$ and

$$R\left(U^l\right) = \frac{\Delta t}{\Delta \xi}\left(\hat{F}^l_{j+\frac{1}{2}} - \hat{F}^l_{j-\frac{1}{2}}\right) - \frac{\Delta t}{\Delta \eta}\left(\hat{G}^l_{k+\frac{1}{2}} - \hat{G}^l_{k-\frac{1}{2}}\right) \tag{3}$$

The numerical flux in ξ for the Harten and Yee non-MUSCL scheme in a pseudo finite volume formulation is

$$\begin{aligned} \hat{F}_{j+\frac{1}{2}} = \frac{1}{2}\Bigg[& \left(\frac{\xi_x}{J}\right)_{j+\frac{1}{2}} (F_j + F_{j+1}) \\ & + \left(\frac{\xi_y}{J}\right)_{j+\frac{1}{2}} (G_j + G_{j+1}) \\ & + \left(\frac{\xi_t}{J}\right)_{j+\frac{1}{2}} (U_j + U_{j+1}) + R_{j+\frac{1}{2}} \Phi_{j+\frac{1}{2}} / J_{j+\frac{1}{2}} \Bigg] \end{aligned} \tag{4}$$

the flux in η is obtained by substituting ξ by η and j by k, respectively.

Φ is a function which contains the flux limiter function which is described in the next section (for details see[10]).

Flux Limiter The flux limiter (g) is a nonlinear function that switches the numerical scheme to first order accuracy in local extrema which occur near discontinuities. The currently implemented limiter is the minmod limiter which may be written in the scalar case as

$$g_j = minmod(\Delta_- u_j, \Delta_+ u_j) \tag{5}$$

where

$$minmod(a,b) = \begin{cases} sign(a)\, min(|a|,|b|) & \text{if } sign(a) = sign(b) \\ 0 & \text{otherwise} \end{cases} \tag{6}$$

and $\Delta_\pm u_j = \pm(u_{j\pm1} - u_j)$.

Grid Coupling To couple the two relatively moving grids a local pointwise method must be found that allows the transport of the mass, momentum and energy fluxes from one grid to the next in time accurate manner [11]. The method must not introduce spurious oscillations nor should it decrease the accuracy of the scheme.

In the presented method sheared cells are used as shown in figure 4. Both grids are locally reconnected as the grid is moving and the metric terms are recalculated. Thus the only error one may expect is due to the local change in the metric terms introduced by these sheared cells.

Boundary Conditions In turbomachinery applications one usually finds four types of boundaries: solid wall, periodicity, inflow and outflow (see also fig. 2).

The solid wall boundary condition is realized via the mirror cell technique [7] and the momentum equation normal to the surface. The motion of the solid boundary has also to be taken into account.

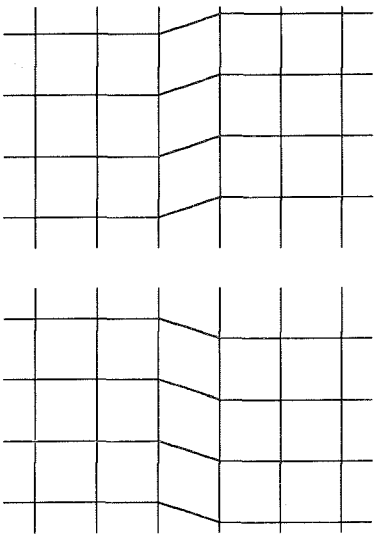

Figure 4: Grid coupling via sheared cells. While the grids are moving relatively slightly sheared cells are formed at each time step. The cells are formed using nearest grid lines.

The periodic and interprocessor boundaries can be prescribed exactly by an overlapping grid.

The inflow and outflow boundary conditions are more difficult to treat, because the prescribed flow is characterized by blade interactions which produce periodic unsteady perturbations. These perturbations have to pass the boundaries without any non-physical reflections. On the other hand additional properties are essential because of the assignment of the interactive simulation system:

- The formulation of the boundary conditions should be accurate in a wide physical range, ie from zero flow and non-moving blades (steady state) up to relative supersonic flow and moving blades (unsteady flow).
- The physical parameters which specify the problem should be altered by manipulating the boundary conditions interactively.

The implemented inflow-outflow boundary conditions combine the non-reflecting treatment with the far field flow values.

The non-reflecting boundary approach is based on non-reflecting boundary-conditions developed by Giles[4]. The formulation which is applicable for steady and unsteady problems is coupled with the occurence of periodic boundaries and therefore particulary suitable for the mentioned flow problem.

Because the flow values at the far-field are not known beforehand they have to be calculated during the integration process, but without violating the linear theory on which the non-reflecting approach is based. They should also perform user specified quantities. The complete implementation is described in more detail in [1].

The currently implementd periodic boundary conditions do not in general allow different pitch to chord ratios to be handled. In special cases where simple multiplicities are used several passages may be simulated to overcome this difficulty. This of course is only advisable in special cases where the number of passages is small.

IV Results

In the following section the results of the simulation of a 2D flow case, the unsteady flow through two cascades moving in opposite direction, will be shown. These cascades represent a typical transonic near tip section of the counter-rotating fan rotor.

The simulation process consists of the start-up and acceleration of the blades prior to the steady operating point of the fan. The far-field boundary conditions at this operating point are:

$$\begin{aligned} T_1|_I &= 288.15K \\ p_1|_I &= 101325.0N/m^2 \\ \alpha_1|_I &= 0^o \\ u|_I &= -241.9m/s \\ u|_{II} &= 120.95m/s \\ M_2|_{II} &= 0.2503 \end{aligned}$$

where the subscribt I denotes values for the first rotor and II denotes values for the second rotor.

Profile Figure 5 shows the transonic profile for both cascades. Typical parameters of this profile are:

- The maximum thickness is 0.05 located at 40% chord length.
- Radius at the trailing edge 0.004.
- Leading edge thickness 0.008.

All variables are related to the chord length.

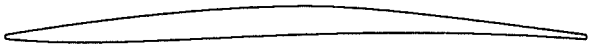

Figure 5: cascade profile

Cascade The first cascade moves downwards while the second one moves upwards. Both pitch to chord ratios are 1 and the stagger angles are 150° for the first and 158° for the second cascade. The steady flow field of a single cascade was investigated in wind tunnel tests at the DLR cologne [13].

Grid A body-fitted structured multiblock grid is used for both cascades. The grid consists of an O-grid around the profile and four H-grids. Latter ones simplifies the handling of the periodic, entry and exit boundary.

The number of grid points is 2440 for each cascade. The formulation of entry and exit boundary conditions allow a location of entry and exit boundary close to the cascades. Therefore the grid within the passage is not too coarse despite the low number of grid points.

The flow solver is parallelized by the idea of domain decomposition as mentioned in section III. For this calculation 32 processors are used. Therefore the complete grid is subdivided into 32 patches which are mapped onto undependly working processors. Figure 6 shows the subdivided multiblock grid.

Calculation Because of the mathematical properties of the Euler equation system —it as an Initial Boundary Value Problem— the calculation has to start with physical correct data. Otherwise the time integration could yield to non-physical results. The only flow field known beforehand is the so called 'zero flow condition'.

Therefore the flow velocity in the complete computational domain is equal zero at time step n= 0 . The simulation process is then started by lowering the far-field pressure at the exit boundary form $\frac{p}{p_{tot}} = 1.0$ to $\frac{p}{p_{tot}} = 0.8$. As a consequence a rarefraction wave propagates from the exit boundary towards the entry boundary. When the rarefraction wave reaches the entry boundary a flow field has established in the complete computational domain (Fig. 7). Then both cascades are accelerated by the same constant rate.

The sequence of the figures 8 to 12 show the pressure

contours at different time levels. The structure of the flow field is characterized by the interaction of waves which are produced by the acceleration process and the waves caused by the initial pressure variation. The 'bubble-like' structures, which can be seen up from figure 9 are typical for this interaction.

Up to nearly 15000 time steps the flow field changes rapidely. Then most of the disturbances are propagated downstream and move out off the computational domain. The resulting flow field becomes periodic in time.

The last figure shows the flow field after 18000 time steps (Fig. 13). The first cascade has zero incidence and a supersonic region on the suction side. The flow field within the second cascade is supersonic and dominated by a strong passage shock which stands at the trailing edge. The extension of the shock indicates a too coarse grid in this region.

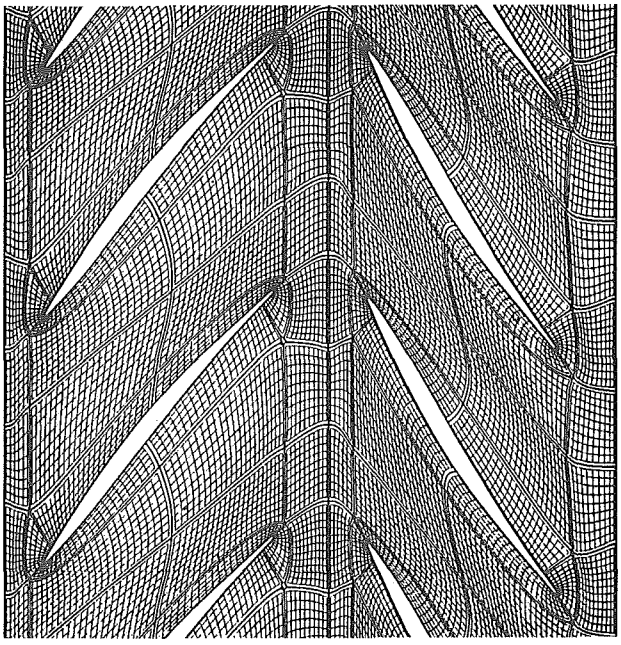

Figure 6: boddy-fitted structured multiblock H-H-O-H-H grid

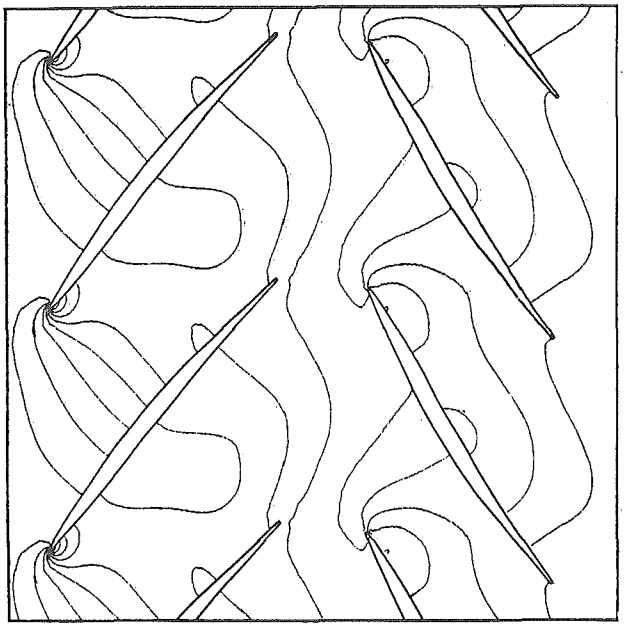

Figure 7: pressure contours time step n = 2000, rarefraction wave reaches the entry boundary

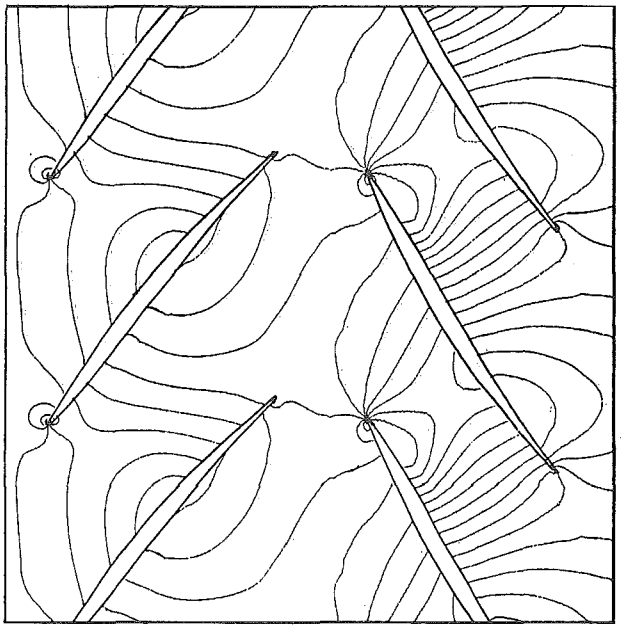

Figure 8: pressure contours time step n = 3500, 1st cascade 40%, 2nd cascade 84% final 'rotational speed'

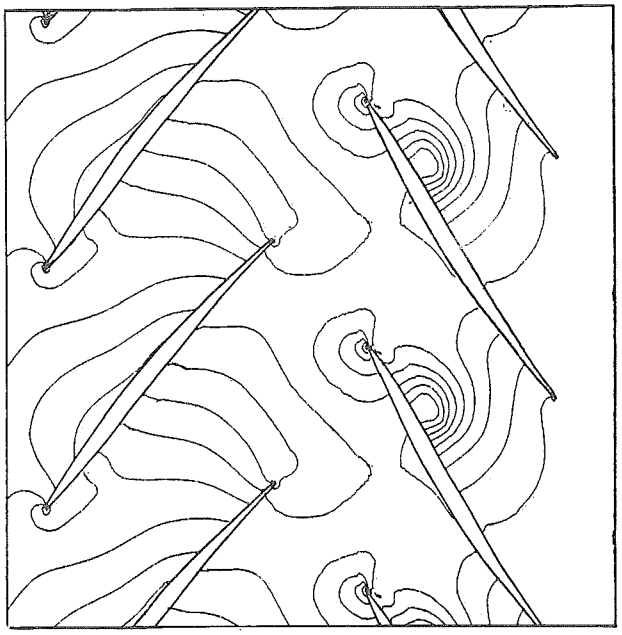

Figure 9: pressure contours time step n = 4000, 1st cascade 60%, 2nd cascade 100% final 'rotational speed'

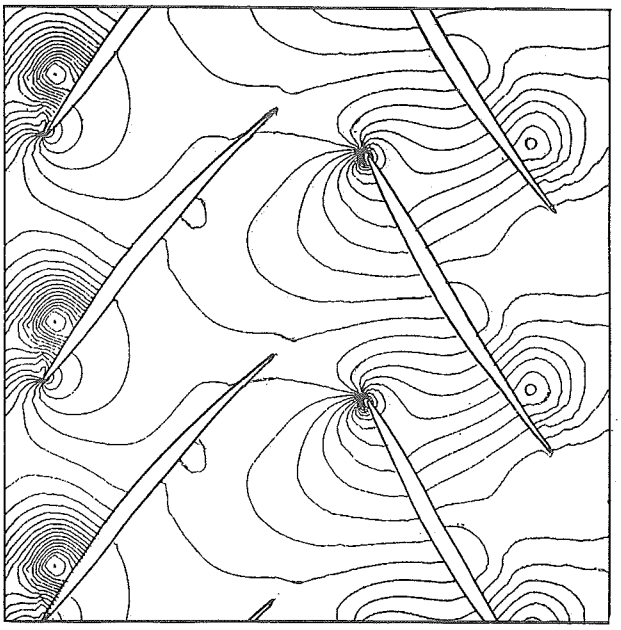

Figure 11: pressure contours time step n = 6500, 1st cascade 76% final 'rotational speed'

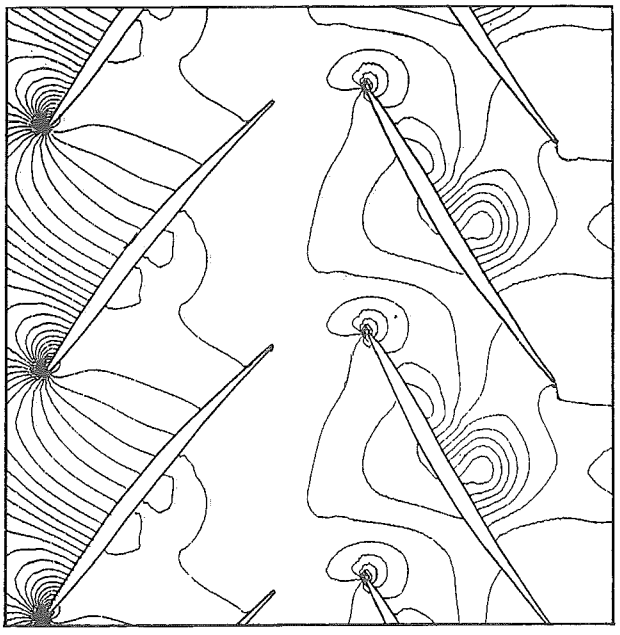

Figure 10: pressure contours time step n = 5500, 1st cascade 68% final 'rotational speed'

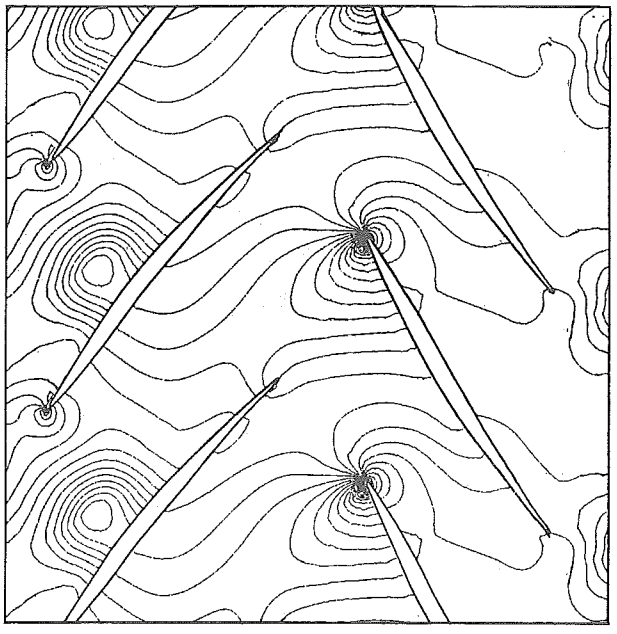

Figure 12: pressure contours time step n = 7500, 1st cascade 84% final 'rotational speed'

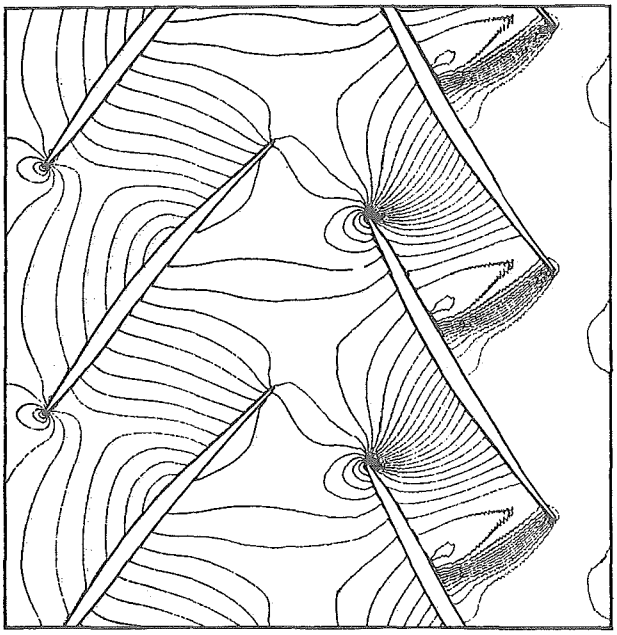

Figure 13: pressure contours time step n = 18000, periodic state is reached

IV Conclusion

An interactive simulation system on a parallel computer is presented. It is under development by the authors to study and analysize the unsteady flow in turbomachinery components.

As an example results of an inviscid calculation of the flow through countermoving cascades are shown.

The results indicate that the formulation of the grid coupling and the implemented solid, entry and exit boundary conditions work well. Further studies for a quantitative study on the accuracy of the scheme will be done.

For the detailed analysis of the flow phenomena the used O-grid around the profiles gives a good resolution of the flow field at the trailing and leading edge regions, but for shocks which occure within the cascade the grid is much too coarse.

Future work will cover the development of a three dimensional system with Navier-Stokes solver for the theoretical investigation of viscid unsteady flow. This can only be achieved by using computers consisting of a few hundered processors.

References

[1] K. ENGEL M. FADEN S. POKORNY, *Implementation of Non-Reflecting Boundary Conditions into an Unsteady Flow Simulation System*, 3.rd International Conference on Numerical Methods for Fluid Dynamics ICFD92, 07-10 April 1992, Reading, UK

[2] S. POKORNY, M. FADEN K. ENGEL *An Integrated Flow Simulation System On A Parallel Computer. Part I: The Basic Idea*, 7.th International Conference on Numerical Methods in Laminar and Turbulent Flow, July 15-19th 1991, Stanford, CA, U.S.A.

[3] M. FADEN, S. POKORNY, K. ENGEL *An Integrated Flow Simulation System On A Parallel Computer. Part II: The Flow Solver*, 7.th International Conference on Numerical Methods in Laminar and Turbulent Flow, July 15-19th 1991, Stanford, CA, U.S.A.

[4] M.B. GILES *Non-Reflecting Boundary Conditions for the Euler Equations*, CFDL-TR-88-1, February 1988.

[5] A. HARTEN *On a class of high-resolution total-variation-stable finite-difference schemes* SIAM J. NUM. ANAL., Vol.21, pp.1-23, 1984.

[6] A. HARTEN, B. ENQUIST, S. OSHER, S. CHAKRAVARTHY *Uniformly High Order Accurate Essentially Non-Oscillatory Schemes III* ICASE Report No. 86-22, 1986

[7] C. HIRSCH *Numerical Computation of Internal and External Flows*, Volume 2, John Wiley & Sons, 1990.

[8] P. L. ROE *Approximate Rieman solvers, parameter vector and difference schemes* Journal Computational Physics, 43, 357-72, 1981.

[9] Y. J. MOON, H. C. YEE *Numerical Simulation by TVD Schemes of Complex Shock Reflections from Airfoils at High Angle of Attack* AIAA-87-0350, AIAA 25th Aerospace Science Meeting, Reno, Nevada, January 12-15, 1987.

[10] H. C. YEE *A class of high-resolution explicit and implicit shock-capturing methods* VKI-Lecture Notes in computational fluid dynamics, 1989.

[11] M. M. RAI *Unsteady Three-Dimensional Navier-Stokes Simulations of Turbine Rotor-Stator Interaction* AIAA Paper No. 87-2058, 1987

[12] C. UPSON, T. FAULHABER *The application Visualiztion System: A Computational Environment for Scientific Visualization* IEEE Computer Graphics & applications, 1989.

[13] A. WEBER
DLR cologne , private comunication